Research Article

Daisuke Akiyama*, Tomoki Mishima, Yoshihiro Okamoto, and Akira Kirishima

Dry synthesis of brannerite (UTi_2O_6) by mechanochemical treatment

https://doi.org/10.1515/htmp-2022-0268
received July 27, 2022; accepted January 06, 2023

Abstract: A powder mixture of UO_2 and TiO_2 was mechanochemically treated in a planetary ball mill under Ar atmosphere for 1 h using a tungsten carbide vial and balls as the milling medium. Such mechanochemical (MC) treatment reduced the crystallinity of UO_2 and TiO_2. The mechanochemically treated powder mixture was heated at 700–1,300°C for 6 h under Ar atmosphere and analyzed by X-ray diffraction analysis, scanning electron microscopy-energy-dispersive X-ray spectroscopy, and X-ray absorption fine structure analysis. For comparison, a UO_2 and TiO_2 mixture without MC treatment was heated and analyzed under the same conditions. UTi_2O_6 did not form below 1,100°C without MC treatment and only the starting materials were observed. At 1,200 and 1,300°C, a small amount of UTi_2O_6 and equal amounts of UTi_2O_6 and UO_2 were formed, respectively. The mechanochemically treated sample produced nearly pure UTi_2O_6 containing small amounts of UO_2 impurities when heated above 900°C for 6 h. UTi_2O_6 was highly crystalline and uniform regardless of the synthesis temperature. It is suggested that the crystallinity of UO_2 and TiO_2 was reduced and the formation of UTi_2O_6 was promoted by MC treatment.

*** Corresponding author: Daisuke Akiyama,** Institute of Multidisciplinary Research for Advanced Materials (IMRAM), Tohoku University, 1-1 Katahira, 2-Chome, Aoba-ku, Sendai 980-8577, Japan, e-mail: d.akiyam@tohoku.ac.jp
Tomoki Mishima: Institute of Multidisciplinary Research for Advanced Materials (IMRAM), Tohoku University, 1-1 Katahira, 2-Chome, Aoba-ku, Sendai 980-8577, Japan; Department of Quantum Science and Energy Engineering, Graduate School of Engineering, Tohoku University, 6-3 Aoba, Aramaki, Aoba-ku, Sendai, 980-8579, Japan
Yoshihiro Okamoto: Materials Sciences Research Center, Japan Atomic Energy Agency, 1-1-1 Kouto, Sayo-cho, Sayo-gun, Hyogo 679-5148, Japan
Akira Kirishima: Institute of Multidisciplinary Research for Advanced Materials (IMRAM), Tohoku University, 1-1 Katahira, 2-Chome, Aoba-ku, Sendai 980-8577, Japan

Keywords: brannerite, uranium titanate, mechanochemical method, dry synthesis

1 Introduction

Brannerite, UTi_2O_6, is a U ore in U deposits. UTi_2O_6 is present in several geological environments such as Elliot Lake (Ontario, Canada) [1,2], Mount Isa (Australia) [3,4], Kirovograd (Ukraine), Crocker Well (Australia) [5], and Domes Region (Zambia) [6] and in some U deposits in the Witwatersrand area (South Africa) [7]. It is commonly produced as an amorphous mineral owing to radiation damage from the alpha decay of U, Th, and their daughter isotopes. It can be recrystallized by heating at approximately 1,000°C [8,9].

UTi_2O_6 is chemically durable and can form solid solutions with alkaline earth elements, rare earth elements, and actinides like Pu and Th. It is a minor phase in titanate-based and pyrochlore-rich Synroc-type ceramics designed for the geological immobilization of excess Pu from nuclear weapons [10]. It was determined that UTi_2O_6 in ceramics incorporates Pu and neutron absorbers like Gd and Hf [11]. Neutron absorbers can overcome potential criticality problems associated with Pu.

Many researchers have reported on the chemical durability and synthesis of UTi_2O_6. The chemical durability of UTi_2O_6 is lower than those of other compounds that form in Synroc, such as pyrochlore and zirconolite, but is higher than that of borosilicate glass which is used for the solidification of high-level radioactive waste solutions [12–14]. The chemical durability of naturally occurring amorphous UTi_2O_6 is approximately 1/10 that of synthesized crystalline UTi_2O_6. However, it is more chemically durable than borosilicate glass used for the solidification of high-level radioactive waste solutions [9].

The synthesis of UTi_2O_6 requires two steps: pretreatment, which involves mixing U and Ti compounds, and heat treatment, which involves the calcination of the mixture. Two types of reported pretreatment processes for the synthesis of UTi_2O_6 are commonly used, *viz.* dry

and wet pretreatments. Dry pretreatment is a simple process that involves mixing and pelleting U and Ti. Wet pretreatment is a complex process in which U and Ti are dissolved, dried, or coprecipitated. The resulting mixture is then calcined and pelletized. The details of the pretreatment processes are provided below.

Dry pretreatment:

- UO_2 and TiO_2 (anatase) powders were mixed in a ball mill and pelletized [15].

Wet pretreatment:

- Uranyl acetate and titanyl sulfate were dissolved in an oxalic acid solution, dried by heating at 200 and 600°C in air and a reducing atmosphere, respectively, and pelletized [16,17].
- Uranyl nitrate and titanium alkoxide were dissolved in water and heated at 200 and 750°C in air. The mixture was then wet-mixed for 16 h and pelletized [18,19].
- Uranyl nitrate or uranyl acetate and titanyl sulfate were dissolved in 1 M oxalic acid and stirred. A concentrated ammonium hydroxide solution was added to raise the pH to 10–11, and the coprecipitation of titanyl hydroxide and uranyl hydroxide occurred. The precipitate was washed twice with an ammonium hydroxide solution at pH 11 and dried at 100°C. After drying, the mixture was calcined at 600°C in air for 5 h [16].

After dry pretreatment, UTi_2O_6 was synthesized by heating at 1,350°C for 300 h in a mixture of 5% CO and 95% CO_2. UTi_2O_6 synthesized using this method contained 0.6 at% unreacted UO_2 [15]. After wet pretreatment, UTi_2O_6 was synthesized by heating at 1,100–1,300°C for 5–96 h or more in an inert or reducing atmosphere. Hussein et al. reported the formation of UTi_2O_6 by heating at 900°C for 5 h in an Ar and 5% H_2 atmosphere, but unreacted UO_2 and TiO_2 was present in the final product. Temperatures exceeding 1,100°C were required to synthesize pure UTi_2O_6 [16]. Wet pretreatment can accelerate the reaction rate and lower the synthesis temperature compared with dry pretreatment. However, wet pretreatment is disadvantageous as a solidification process for radioactive waste because of its complicated operation and the generation of radioactive liquid waste. Furthermore, because U in solution is hexavalent, it is necessary to use reductants (such as H_2 gas) during heat treatment to synthesize UTi_2O_6, which is composed of tetravalent U. Alternatively, dry pretreatment is a simple process that does not generate radioactive liquid waste or require a reductant (H_2 gas). However, dry pretreatment requires an extended reaction time and higher reaction temperature compared with wet pretreatment.

In this study, we aimed to reduce the heating time and temperature for the synthesis of UTi_2O_6 by dry pretreatment using mechanochemical (MC) treatment. Dry MC treatment uses a planetary ball mill to improve the reactivity by rotating a hard ball and raw powder in a cylindrical container that applies mechanical energy. UO_2 and TiO_2 (rutile) powders were MC treated at a molar ratio of U:Ti = 1:2 and pelletized. The pellets were heated at 700–1300°C for 6 h in an Ar atmosphere to investigate the formation temperature of UTi_2O_6. To confirm the effect of MC treatment, UO_2 and TiO_2 pellets without MC treatment were heat-treated under the same conditions as when MC treatment was applied. After MC treatment, the crystal structures of the synthesized UTi_2O_6 were analyzed by X-ray diffraction (XRD) analysis, scanning electron microscopy-energy-dispersive X-ray spectroscopy (SEM-EDX), and X-ray absorption fine structure (XAFS) analysis to determine the reaction mechanism.

2 Materials and methods

2.1 Materials

UO_2 was prepared by reducing U_3O_8 at 1,000°C for 4 h in an Ar and 10% H_2 atmosphere at a gas flow rate of 60 mL·min^{-1}. Rutile TiO_2 powder (99% purity) was a special grade reagent obtained from FUJIFILM Wako Pure Chemical Corporation.

2.2 Synthesis

2.2.1 Mechanochemical treatment

A planetary ball mill (Fritsch Pulverisette-7) was used to mill UO_2 and TiO_2 powders. A tungsten carbide pot (inner volume: 45 mL) was loaded with 0.8 g of the powder mixture and 10 tungsten carbide balls (φ10 mm). The milling pot was transferred to an acrylicvacuum glove box. The glove box was evacuated and refilled with Ar (G1 grade, 99.9999%) three times to make the internal atmosphere inert. The milling pot and its lid were packed with silicone rubber before being removed from the glove box. The boundary between the milling pot and lid was sealed with aluminum tape to maintain an inert atmosphere. After setting a pair of milling pots in a planetary mill, the mill was rotated at 700 rpm at room temperature. The milling operation was interrupted every 5 min for 1 h to avoid overheating owing to MC treatment; hence, the total milling time was 30 min. Finally, the pot was left

to cool for approximately 30 min and the mixed sample was removed from the pot.

Without MC treatment, UO_2 and TiO_2 powders were mixed in a mortar.

2.2.2 Heat treatment

The MC-treated mixture was pelletized (φ7 mm) and placed on an alumina boat. The sample was sintered under an Ar (G1 grade, 99.9999%) atmosphere at 700–1,300°C for 6 h. For comparison, mixtures without MC treatment were heated using the same procedure as when MC treatment was applied.

2.3 XRD

XRD patterns were obtained using an X-ray diffractometer (Rigaku Mini Flex 600) with Ni-filtered Cu Kα radiation operated at 40 kV and 15 mA. Diffraction patterns were collected in the 2θ range of 10–140° with a step interval of 0.02° at a scan rate of $5°\cdot min^{-1}$.

2.4 SEM-EDX

A Hitachi VP-SEM SU1510 by Hitachi High Technologies Corporation was used to perform SEM. EDS was carried out using an EMAX EX-250, X-act by Oxford Instruments.

2.5 XAFS

XAFS measurements were performed at the BL-27B station of the Photon Factory in KEK, Tsukuba, Japan. An X-ray beam monochromatized by Si (111) double crystals is available at the beamline [20]. XAFS spectra of the U L_3-edge (E_0 = 17.166 keV) with energies of 16.865–17.874 keV were collected using this transmission method, while those of a Ti K-edge (E_0 = 4.966 keV) with energies of 4.780–5.856 keV were obtained using a fluorescence method. X-ray energy was calibrated using the standard oxides UO_2 and U_3O_8 for the U L_3-edge and TiO_2 for the Ti K-edge. XAFS data were analyzed using WinXAS ver. 3.2 software [21] to obtain the extended XAFS (EXAFS) k^3 function (k) and the Fourier transform magnitude (|FT|). Structural parameters such as the coordination number and interatomic distance were obtained using the curve-fitting procedure in WinXAS. The correction parameters required in the fitting analysis, namely the phase shift and backscattering amplitude, were obtained from the XAFS simulation software FEFF Ver. 8.4.

3 Results and discussion

3.1 Mechanochemical treatment

Figure 1 shows the XRD patterns of the UO_2 and TiO_2 mixture before and after MC treatment. XRD measurements were performed on UO_2 and TiO_2 to determine the peaks present before MC treatment. A broadening of the UO_2 and TiO_2 peaks was noted after MC treatment. This suggests that the crystallinity of UO_2 and TiO_2 decreased. The lattice constant of UO_2 changed from 5.471 to 5.462 Å after MC treatment. The minimal oxidation of UO_2 may be caused by the small amount of remaining oxygen in the milling pot. No UTi_2O_6 peaks were observed after MC treatment.

Figure S1 shows that the mixture of UO_2 and TiO_2 before MC treatment has separate distributions of UO_2 and TiO_2 of a few microns. As shown in Figure 2(a), the particle size in the mixture after MC treatment was less than a few microns. From Figure 2(b) and (c), it can be observed that U and Ti are similarly distributed. It was concluded that MC treatment reduced the crystallinity of UO_2 and TiO_2 and that they became a homogeneous mixture consisting of fine particles.

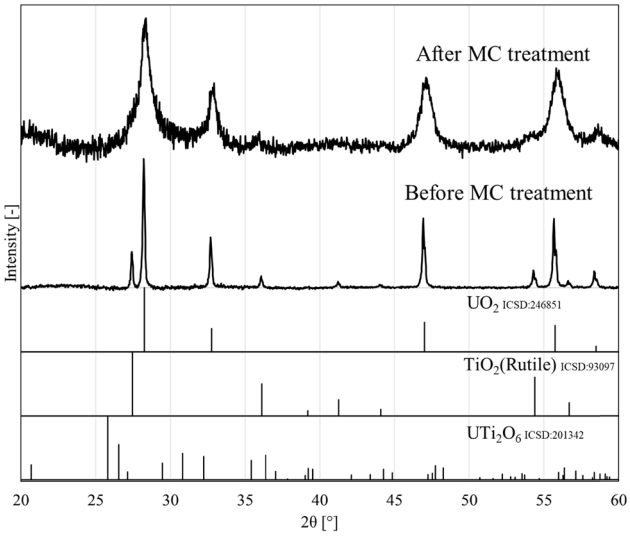

Figure 1: X-ray diffraction patterns of UO_2 and TiO_2 mixtures before and after MC treatment.

3.2 Heat treatment of the mixture

3.2.1 UTi_2O_6 synthesis without MC treatment

A UO_2 and TiO_2 mixture that was not MC treated was heated. Figure 3 shows XRD measurements of samples heated at 1,000–1,300°C. Below 1,100°C, only the UO_2 and TiO_2 peaks of the starting materials were observed and no UTi_2O_6 peaks were present. At 1,200°C, the main phases were UO_2 and TiO_2, whereas the UTi_2O_6 phase was observed as a minor phase with small XRD peak intensities. At 1,300°C, similar amounts of UTi2O6 phase and unreacted UO_2 and TiO_2 phases were observed. Rietveld analysis was used to quantitatively analyze the XRD pattern of the sample heated at 1,300°C. The abundances of the UO_2 and UTi_2O_6 phases were 59 ± 1 and 41 ± 2 at%, respectively. UTi_2O_6 formed without MC treatment at 1,300°C, but the heating time needed to be prolonged to obtain pure UTi_2O_6.

3.2.2 UTi_2O_6 synthesis with MC treatment

After MC treatment, the UO_2 and TiO_2 mixture was heated. Figure 4 shows XRD patterns of samples heated at 700–1,300°C. Below 800°C, only the UO_2 and TiO_2 peaks of the starting materials were observed and no UTi_2O_6 was formed. At 900°C, the UTi_2O_6 phase coexisted with approximately 22 at% UO_2. Above 1,000°C, nearly pure UTi_2O_6 phase was formed with less than 11 at%

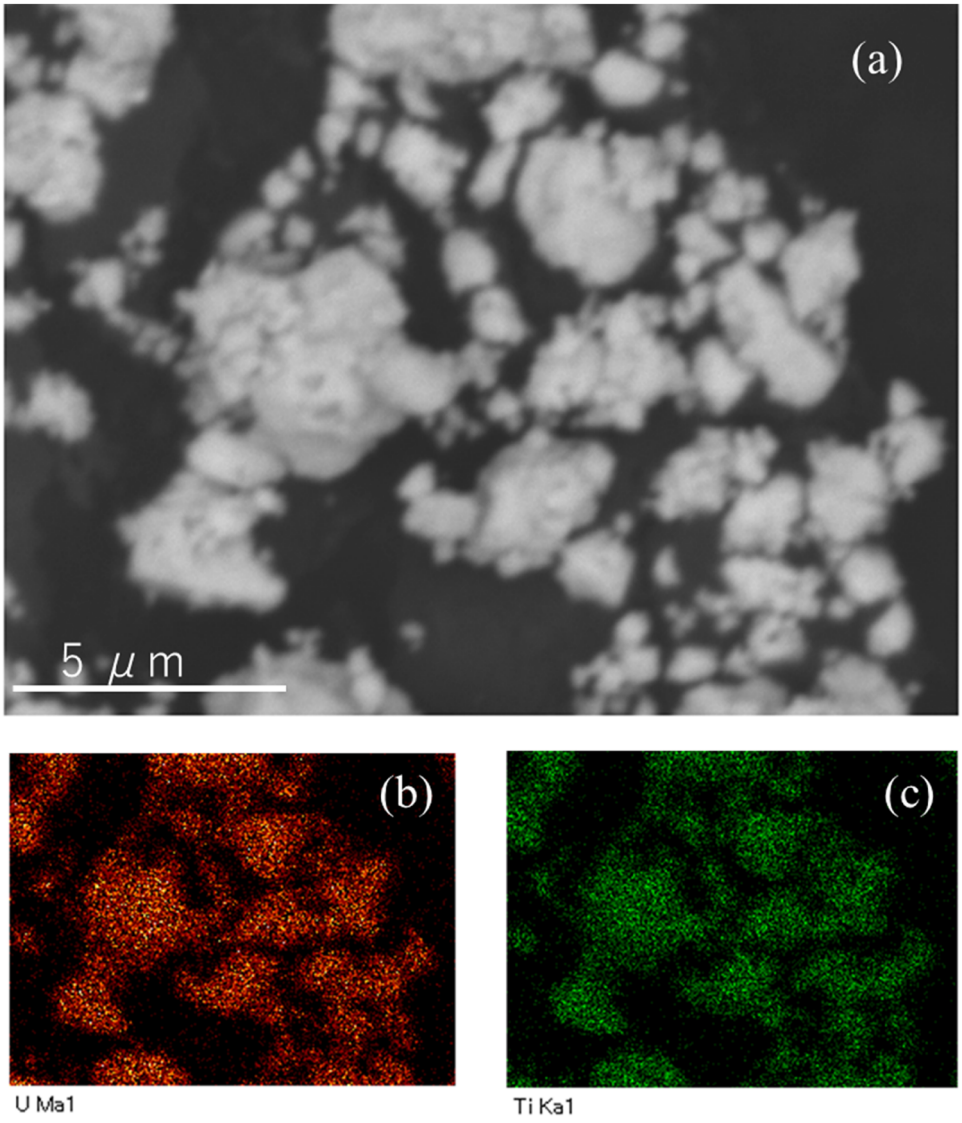

Figure 2: SEM-EDX of UO_2 and TiO_2 mixtures after MC treatment. (a) Scanning electron microscopy image (BSE, ×8,000), (b) U distribution, and (c) Ti distribution of a UO_2 and TiO_2 mixture.

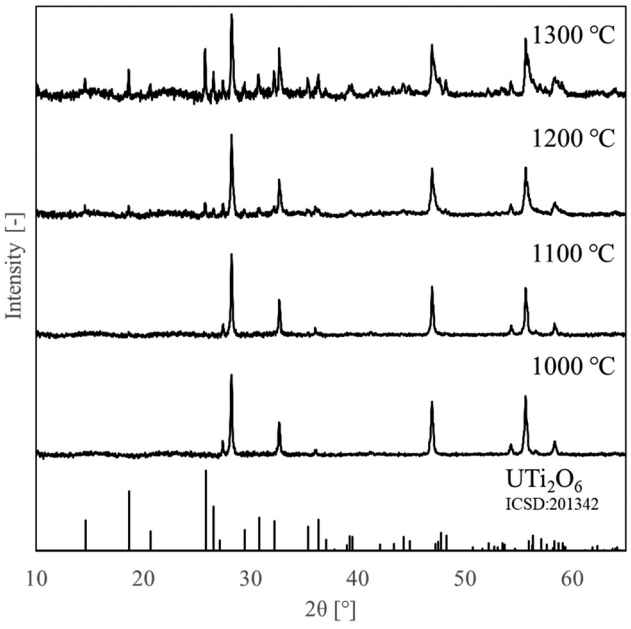

Figure 3: X-ray diffraction patterns of a UO_2 and TiO_2 mixture without MC treatment after being heated.

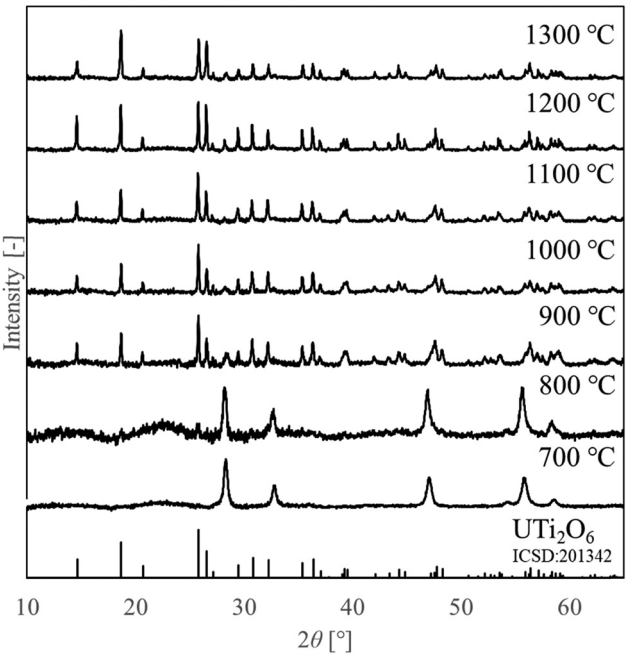

Figure 4: X-ray diffraction patterns of a UO_2 and TiO_2 mixture with MC treatment after being heated.

coexistence of UO_2. The lattice parameters of the formed UTi_2O_6 are listed in Table 1. From Table 1, it was confirmed that the lattice parameters remained consistent. This suggests that a comparable UTi_2O_6 phase was formed regardless of the heating temperature.

Figure 5 shows the SEM-EDS analysis of UTi_2O_6 synthesized by heat treatment at 1,100°C. Figure 5(a) indicates that the particle size of the mixture remained consistent at less than a few microns before and after heat treatment. Figure 5(b) and (c) shows that U and Ti were similarly distributed before and after heating.

3.3 XAFS analysis

Figure 6 shows U L_3 X-ray absorption near the edge structure (XANES) spectra of UO_2, U_3O_8, a UO_2 and TiO_2 mixture that was MC treated without heating and UTi_2O_6 synthesized at 1,300°C with MC treatment. Based on Figure 6, it was deduced that the U in the MC-treated UO_2 and TiO_2 mixture and synthesized UTi_2O_6 were tetravalent because their white-line energies were similar to that of UO_2, which is the standard material of tetravalent U. The XANES spectra of UO_2 and the UO_2 and TiO_2 mixture were very similar, which indicated that the crystal structure of UO_2 was maintained after MC treatment. The XAFS spectra of UTi_2O_6 and UO_2 indicated that alternative crystals to UO_2 formed in the synthesized UTi_2O_6 that was MC treated.

Figure 7 shows EXAFS and FT magnitude functions of the U L_3- and Ti K-edges of UO_2, the MC-treated UO_2 and TiO_2 mixture, and UTi_2O_6 synthesized at 900 and 1,300°C. The U L_3 EXAFS function in Figure 7(a-1) shows that the spectrum of UO_2 did not change significantly after MC treatment. This indicates that the crystal structure of UO_2 remained consistent. There is a considerable

Table 1: Lattice parameters of the synthesized UTi_2O_6 and remaining UO_2 after heat with MC treatment

Heating temperature (°C)	Lattice parameter of UTi_2O_6			Remaining UO_2 (at%)
	a (Å)	*b* (Å)	*c* (Å)	
900	9.820 ± 0.007	3.7700 ± 0.0010	6.926 ± 0.005	22.0 ± 3.7
1,000	9.813 ± 0.004	3.7722 ± 0.0017	6.927 ± 0.003	11.1 ± 1.8
1,100	9.825 ± 0.004	3.7745 ± 0.0018	6.935 ± 0.003	3.0 ± 0.6
1,200	9.824 ± 0.003	3.7728 ± 0.0012	6.931 ± 0.002	8.9 ± 1.2
1,300	9.817 ± 0.002	3.7686 ± 0.0009	6.923 ± 0.002	5.8 ± 0.4

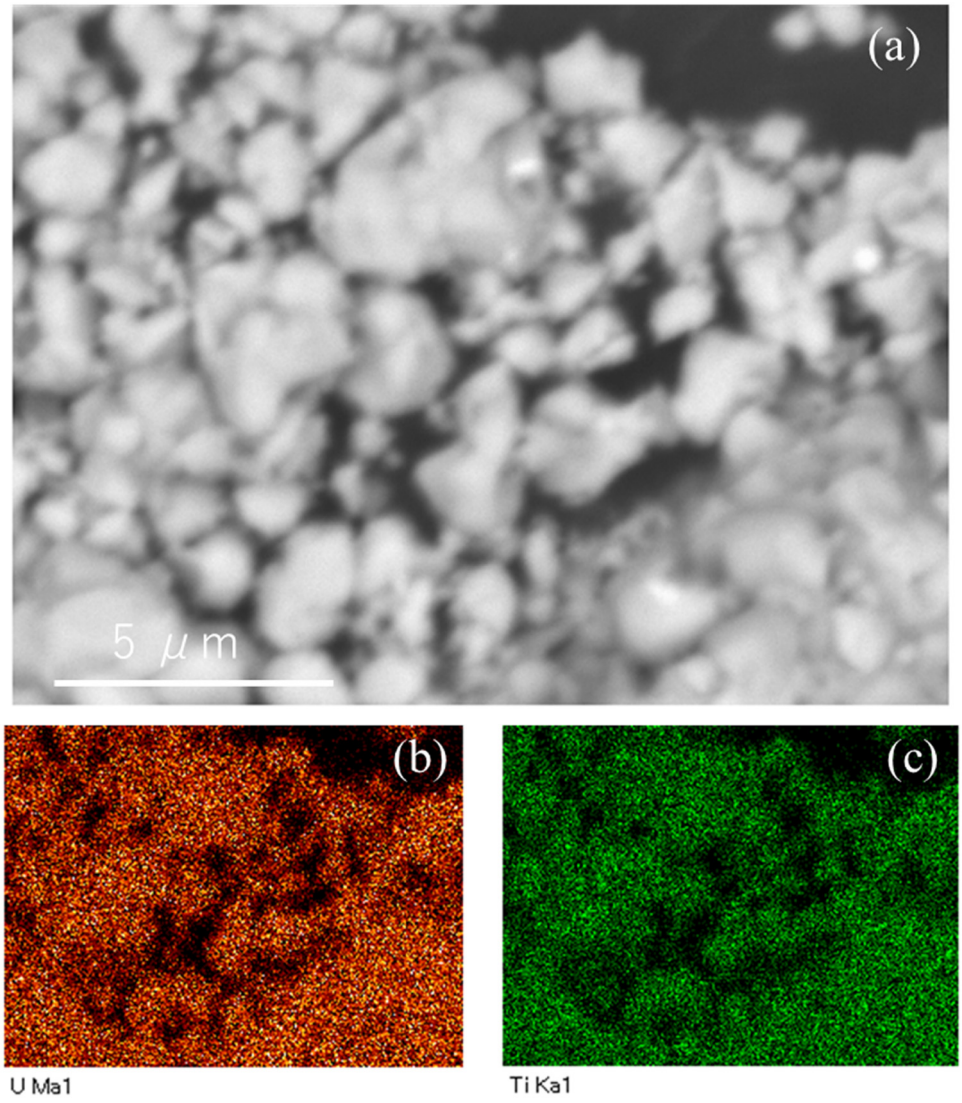

Figure 5: SEM-EDX analysis after MC treatment of a UO_2 and TiO_2 mixture at 1,100°C. (a) Scanning electron microscopy image (BSE, ×8,000), (b) U distribution, and (c) Ti distribution of a UO_2 and TiO_2 mixture.

difference between the spectra of UTi_2O_6 and UO_2. The U L_3-edge FT magnitude function in Figure 7(a-2) shows that the U–O and U–U bond distances in the first and second coordination spheres remained unchanged after UO_2 was MC treated. However, the peak intensity corresponding to U–U decreased. This suggests that the crystallinity of UO_2 has decreased. The U–O distances of UTi_2O_6 and UO_2 are the same. However, the peak corresponding to the U–U distance in the UTi_2O_6 spectrum disappeared. Structural parameters, such as the coordination number and interatomic distance, were calculated through the curve-fitting analysis of the FT function (Table 2). The U–O distance and coordination number in UO_2 remained unchanged after MC treatment. The increased Debye–Waller factor value indicated that MC treatment caused the crystallinity to decrease. The U–O bond lengths in UTi_2O_6 are (1) two-coordinated $U–O_1$ = 2.252 ± 0.002, (2) four-coordinated $U–O_2$ = 2.296 ± 0.001, and (3) two-coordinated $U–O_3$ = 2.824 ± 0.002 Å [22] (Figure S2). Curve-fitting analysis was performed for two-component systems with short-distance U–O bonds (six-coordination) for (1) and (2), and long-distance U–O bonds (two-coordination) for (3). The results of the analysis are shown in Table 2. The local structure of UTi_2O_6 is consistent with reported U–O bond distances and coordination numbers. There were no significant changes to the local structure of U in UTi_2O_6 synthesized at 900 and 1,300°C.

Similar to UO_2, the Ti K EXAFS function in Figure 7(a-2) indicated that the TiO_2 spectrum did not change significantly

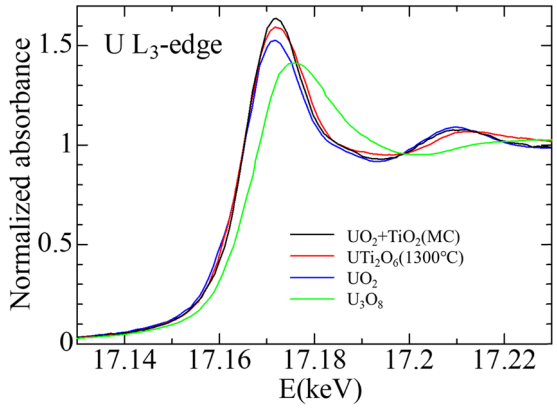

Figure 6: U L_3-edge X-ray absorption near the edge structure spectra of UO_2, U_3O_8, a UO_2 and TiO_2 mixture with MC treatment, and UTi_2O_6 synthesized at 1,300°C.

Table 2: Structural parameters: coordination number *N*, interionic distance $r_{(U-O)}$, Debye–Waller factor σ^2 in UO_2, UO_2 and TiO_2 mixture with MC treatment, and UTi_2O_6 synthesized at 900 and 1,300°C by U L_3-edge XAFS

Sample	S_0^2	*N*	r_{U-O} (Å)	σ^2 (Å^2)
UO_2	0.95	8.2	2.343	0.00663
UO_2 and TiO_2 (MC)	0.95	8.1	2.321	0.01120
UTi_2O_6 (900°C)	0.95	5.9	2.277	0.00639
		2.0	2.832	0.00950
UTi_2O_6 (1,300°C)	0.95	6.0	2.266	0.00452
		2.0	2.815	0.00879

after MC treatment. However, the amplitude of the spectra slightly decreased. This suggests that the crystallinity of TiO_2 decreased. The spectra of UTi_2O_6 were significantly different from those of TiO_2 after MC treatment. The Ti K-edge FT magnitude function in Figure 7 shows that the bond distances of Ti-O and Ti-Ti in the first and second coordination spheres remained unchanged after TiO_2 was MC treated. However, the peak intensity corresponding to Ti-Ti decreased. This suggests that MC treatment caused the crystallinity of TiO_2 to decrease. The Ti-Ti peak observed in TiO_2 disappeared in UTi_2O_6.

3.4 Evaluation of the crystal structures in the UTi_2O_6 synthesis process

XRD results showed that the crystal structures of UO_2 and TiO_2 were maintained when a UO_2 and TiO_2 mixture was MC treated, but the relative intensity of the peaks

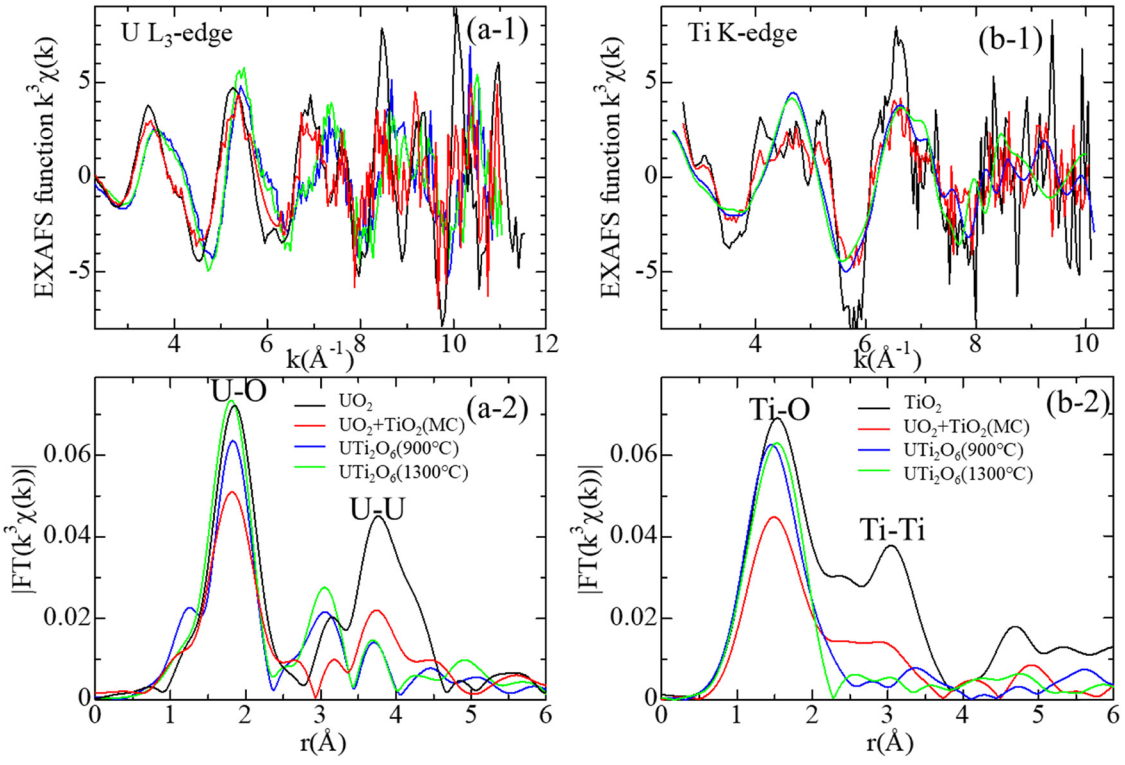

Figure 7: (1) EXAFS and (2) FT magnitude functions of the (a) U L_3- and (b) Ti K-edges of UO_2, TiO_2, a UO_2, and TiO_2 mixture with MC treatment, and UTi_2O_6 synthesized at 900 and 1,300°C.

decreased and broadened. The SEM-EDX results show that MC treatment of mixed samples of UO_2 and TiO_2 resulted in a similar distribution of U and Ti. These results indicate that MC treatment of the UO_2 and TiO_2 mixture reduces the crystallinity of UO_2 and TiO_2. However, no chemical reactions occur and U and Ti exists as separate phases. The results in Table 1 and Figure 7 confirm that the lattice parameter and local structures of U and Ti in UTi_2O_6 remains unchanged regardless of the heating temperature. This reveals that high crystalline UTi_2O_6 can be synthesized by MC pretreatment and heat treatment at 900°C. The reaction temperature (900°C) is similar to that required for recrystallization of naturally existing amorphous UTi_2O_6 (900°C). The formation temperature of UTi_2O_6 exceeded 1,200°C without MC treatment and the formation rate of UTi_2O_6 was faster with MC treatment. The faster reaction rates of UO_2 and TiO_2 with MC treatment are potentially caused by increasing contact points between UO_2 and TiO_2. The contact points increased because the UO_2 and TiO_2 particles are finer and more uniformly mixed and their surfaces are more activated. The lower formation temperature of UTi_2O_6 may be attributed to the lower activation energy of UTi_2O_6 formation owing to the lower crystallinity of UO_2 and TiO_2. Approximately 22 at% of UO_2 remained as impurities when the UO_2 and TiO_2 mixture was heat-treated at 900°C, and less than 11 at% of UO_2 remained at 1,000°C or higher. It is assumed that the formation reaction did not go to completion in the case of heat treatment at 900°C for 6 h. The surface of UO_2 particles was partially oxidized by MC treatment, which prevented the formation of $U^{IV}Ti_2O_6$. Hence, approximately 11 at% of UO_2 remained after heat treatment at 1,000°C or higher, regardless of the reaction temperature.

4 Conclusions

MC treatment of a powder mixture of UO_2 and TiO_2 reduced their crystallinity. UTi_2O_6 with 22 at% and <11 at% impurities were synthesized from this mixture in an Ar atmosphere by heat treatment at 900 and >1,000°C, respectively, for 6 h. The synthesized UTi_2O_6 crystals had consistent crystal structures, regardless of the synthesis temperature (900–1,300°C). Compared with the previously reported dry process that required a reaction temperature of 1,350°C for 300 h, the proposed process of UTi_2O_6 synthesis via MC treatment significantly lowered the synthesis temperature by 450°C and shortened the synthesis time by 294 h. However, small amounts of UO_2 impurities remained in the final product. In conclusion, MC treatment enabled the synthesis of nearly pure UTi_2O_6 at considerably lower temperatures, shorter reaction times, and without reductants compared to previously reported synthesis methods.

Acknowledgments: This study was supported by JSPS KAKENHI (Grant Numbers JP17K14908 and JP20K15203). A part of this study was also supported by the "Dynamic Alliance for Open Innovation Bridging Human, Environment and Materials" of the Ministry of Education, Culture, Sports, Science and Technology of Japan (MEXT). This work was approved by the Photon Factory Program Advisory Committee (proposal number 2021G656). We would like to thank Editage (www.editage.com) for English language editing.

Funding information: JSPS KAKENHI (Grant Numbers JP17K14908 and JP20K15203) and "Dynamic Alliance for Open Innovation Bridging Human, Environment and Materials" of the Ministry of Education, Culture, Sports, Science and Technology of Japan (MEXT).

Author contributions: Daisuke Akiyama: conceptualization, methodology, writing – original draft, writing – review and editing, sample synthesis; Tomoki Mishima: sample synthesis, XRD analysis, SEM-EDX analysis, data curation; Yoshihiro Okamoto: XAFS experiment, data curation; and Akira Kirishima: conceptualization, writing – original draft.

Conflict of interest: The authors state no conflict of interest.

References

[1] Larocque, E. and E. Pakkala. Current leaching and product recovery practice at Denison-mines-limited. *CIM Bulletin*, Vol. 72, 1979, pp. 172–176.
[2] Hester, K. D. Current developments at Rio-Algom, Elliot-Lake. *CIM Bulletin*, Vol. 72, 1979, pp. 181–188.
[3] Wilde, A., A. Otto, J. Jory, C. MacRae, M. Pownceby, N. Wilson, et al. Geology and mineralogy of uranium deposits from Mount Isa, Australia: implications for albitite uranium deposit models. *Minerals*, Vol. 3, 2013, pp. 258–283.
[4] Pownceby, M. I. and C. Johnson. Geometallurgy of Australian uranium deposits. *Ore Geology Reviews*, Vol. 56, 2014, pp. 25–44.
[5] Gilligan, R. and A. N. Nikoloski. The extraction of uranium from brannerite - A literature review. *Minerals Engineering*, Vol. 71, 2015, pp. 34–48.
[6] Eglinger, A., A. Tarantola, C. Durand, C. Ferraina, O. Vanderhaeghe, A. S. André-Mayer, et al. Uranium mobilization by fluids associated with Ca-Na metasomatism: A P-T-t record of fluid-rock interactions during Pan-African metamorphism (Western Zambian Copperbelt). *Chemical Geology*, Vol. 386, 2014, pp. 218–237.

[7] Lottering, M. J., L. Lorenzen, N. S. Phala, J. T. Smit, and G. A. C. Schalkwyk. Mineralogy and uranium leaching response of low grade South African ores. *Minerals Engineering*, Vol. 21, 2008, pp. 16–22.

[8] Charalambous, F. A., R. Ram, M. I. Pownceby, J. Tardio, and S. K. Bhargava. Chemical and microstructural characterisation studies on natural and heat treated brannerite samples. *Minerals Engineering*, Vol. 39, 2012, pp. 276–288.

[9] Zhang, Y., G. R. Lumpkin, H. Li, M. G. Blackford, M. Colella, M. L. Carter, et al. Recrystallisation of amorphous natural brannerite through annealing: The effect of radiation damage on the chemical durability of brannerite. *Journal of Nuclear Materials*, Vol. 350, 2006, pp. 293–300.

[10] Yudintsev, S. V., S. V. Stefanovsky, M. S. Nikol'skii, O. I. Stefanovskaya, and B. S. Nikonov. Brannerite, UTi_2O_6: Crystal chemistry, synthesis, properties, and use for actinide waste immobilization. *Radiochemistry* (*London*), Vol. 58, 2016, pp. 333–348.

[11] Yudintsev, S. V., S. V. Stefanovsky, O. I. Stefanovskaya, B. S. Novikov, and M. S. Nikol'skii. Phase distribution of uranium in matrices for immobilization of the rare earth–actinide fraction of high-level waste. *Radiochemistry* (*London*), Vol. 57, 2015, pp. 640–651.

[12] Lumpkin, G.R. Ceramic waste forms for actinides. *Elements*, Vol. 2, 2006, pp. 365–372.

[13] Wellman, D. M., J. P. Icenhower, and W. J. Weber. Elemental dissolution study of Pu-bearing borosilicate glasses. *Journal of Nuclear Materials*, Vol. 340, 2005, pp. 149–162.

[14] Weber, W. J., A. Navrotsky, S. Stefanovsky, E. R. Vance, and E. Vernaz. Materials science of high-level nuclear waste immobilization. *MRS Bulletin*, Vol. 34, 2009, pp. 46–53.

[15] Donaldson, M. H., R. Stevens, B. E. Lang, J. Boerio-Goates, B. F. Woodfielda, R. L. Putnam, et al. Heat capacities and absolute entropies of UTi_2O_6 and $CeTi_2O_6$. *Journal of Thermal Analysis and Calorimetry*, Vol. 81, 2005, pp. 617–625.

[16] Hussein, A., J. Tardio, and S. Bhargava. Synthesis and Dissolution Studies of Brannerite, a Uranium Containing Mineral. *Chemeca 2008: Towards a Sustainable Australasia*, 2008, pp. 630–640.

[17] Charalambous, F. A., R. Ram, S. McMaster, J. Tardio, and S. K. Bhargava. An investigation on the dissolution of synthetic brannerite (UTi2O6). *Hydrometallurgy*, Vol. 139, 2013, pp. 1–8.

[18] Lutze, W. and R. C. Ewing. *Radioactive waste forms for the future*, Elsevier, 1988.

[19] Vance, E. R., J. N. Watson, M. L. Carter, R. A. Day, and B. D. Begg. Crystal chemistry and stabilization in air of brannerite, UTi_2O_6. *Journal of the American Ceramic Society*, Vol. 84, 2001, pp. 141–144.

[20] Konishi, H., A. Yokoya, H. Shiwaku, H. Motohashi, T. Makita, Y. Kashihara, et al. Synchrotron radiation beamline to study radioactive materials at the photon factory. *Nuclear Instruments and Methods in Physics Research Section A: Accelerators, Spectrometers, Detectors and Associated Equipment*, Vol. 372, 1996, pp. 322–332.

[21] Ressler, T. WinXAS: A Program for X-ray absorption spectroscopy data analysis under MS-windows. *Journal of Synchrotron Radiation*, Vol. 5, 1998, pp. 118–122.

[22] Szymanski, J. T. and J. D. Scott. A crystal-structure refinement of synthetic brannerite, UTi_2O_6, and its bearing on rate of alkaline-carbonate leaching of brannerite in Ore. *Canadian Mineralogist*, Vol. 20, 1982, pp. 271–280.